Published OnlineFirst December 12, 2017; DOI: 10.1158/0008-5472.CAN-17-2644

Translational Science

Cancer Research

# Targeting CDK6 and BCL2 Exploits the "MYB Addiction" of Ph$^+$ Acute Lymphoblastic Leukemia

Marco De Dominici[1], Patrizia Porazzi[1], Angela Rachele Soliera[2], Samanta A. Mariani[1], Sankar Addya[1], Paolo Fortina[1], Luke F. Peterson[3], Orietta Spinelli[4], Alessandro Rambaldi[4], Giovanni Martinelli[5], Anna Ferrari[5], Ilaria Iacobucci[5], and Bruno Calabretta[1]

## Abstract

Philadelphia chromosome–positive acute lymphoblastic leukemia (Ph$^+$ ALL) is currently treated with BCR-ABL1 tyrosine kinase inhibitors (TKI) in combination with chemotherapy. However, most patients develop resistance to TKI through BCR-ABL1–dependent and –independent mechanisms. Newly developed TKI can target Ph$^+$ ALL cells with BCR-ABL1–dependent resistance; however, overcoming BCR-ABL1–independent mechanisms of resistance remains challenging because transcription factors, which are difficult to inhibit, are often involved. We show here that (i) the growth of Ph$^+$ ALL cell lines and primary cells is highly dependent on MYB-mediated transcriptional upregulation of CDK6, cyclin D3, and BCL2, and (ii) restoring their expression in MYB-silenced Ph$^+$ ALL cells rescues their impaired proliferation and survival. Levels of MYB and CDK6 were highly correlated in adult Ph$^+$ ALL ($P = 0.00008$). Moreover, Ph$^+$ ALL cells exhibited a specific requirement for CDK6 but not CDK4 expression, most likely because, in these cells, CDK6 was predominantly localized in the nucleus, whereas CDK4 was almost exclusively cytoplasmic. Consistent with their essential role in Ph$^+$ ALL, pharmacologic inhibition of CDK6 and BCL2 markedly suppressed proliferation, colony formation, and survival of Ph$^+$ ALL cells *ex vivo* and in mice. In summary, these findings provide a proof-of-principle, rational strategy to target the MYB "addiction" of Ph$^+$ ALL.

**Significance:** MYB blockade can suppress Philadelphia chromosome-positive leukemia in mice, suggesting that this therapeutic strategy may be useful in patients who develop resistance to imatinib and other TKIs used to treat this disease. *Cancer Res; 78(4); 1097–109. ©2017 AACR.*

## Introduction

B-cell acute lymphoblastic leukemia (ALL) is a molecularly heterogeneous malignancy with <50% 5-year overall survival in adults (1–3). The Philadelphia chromosome (Ph) is the most common cytogenetic abnormality in adult ALL with an incidence of approximately 30% (4, 5). Standard chemotherapy has a modest impact on long-term survival of Ph$^+$ ALL patients, and only bone marrow transplantation extends long-term survival in 40% to 60% of cases (6). Treatment with the tyrosine kinase inhibitor (TKI) imatinib and chemotherapy has significantly improved the outcome of Ph$^+$ ALL patients (7). However, resistance to imatinib and second-generation TKI develops rapidly in most Ph$^+$ ALL patients (8), probably because of secondary mutations in transformed B-cell progenitors (9, 10) due to aberrant RAG-dependent recombination and/or AID-dependent somatic hypermutation (11–13). Thus, inhibiting the BCR-ABL1 kinase fails to eradicate most Ph$^+$ ALL cell clones due to the activation of BCR-ABL1–dependent and –independent pathways that need to be targeted for an effective treatment.

We and others have identified transcription factors (TF) whose expression/activity is required for BCR-ABL1–dependent leukemogenesis (14–18). In particular, BCR-ABL1–transformed myeloid and lymphoid cells rely on MYB expression more than the normal counterpart (15, 18), supporting the concept that certain leukemic cells are "addicted" to MYB (19–21). This concept was validated in a model of MLL-AF9 AML (22), in which partial and transient suppression of MYB expression phenocopied MLL-AF9 withdrawal, eradicating an aggressive leukemia with no effects on normal myelopoiesis.

Targeting MYB or relevant protein interactions essential for its activity is an attractive strategy to exploit the MYB dependence of BCR-ABL1–transformed B cells. However, it is inherently difficult to specifically target MYB or its partner proteins, as recently identified MYB inhibitors may also function through MYB-independent mechanisms. For example, parthenolide inhibited TF activity of MYB and viability of Ph$^+$ K562 cells (23); however, this drug has multiple mechanisms of action (24, 25), suggesting that its effects may be, in part, MYB-independent. Naphthol AS-E phosphate and celastrol block the interaction between the MYB transactivation domain and the KIX domain of p300, which is required for MYB function (26, 27). However, naphthol AS-E phosphate induces apoptosis more rapidly and effectively than MYB silencing (26),

[1]Department of Cancer Biology, Sidney Kimmel Cancer Center, Thomas Jefferson University, Philadelphia, Pennsylvania. [2]Department of Diagnostic, Clinical Medicine and Public Health, University of Modena, Modena, Italy. [3]Division of Hematology and Oncology, Department of Internal Medicine, University of Michigan, Ann Arbor, Michigan. [4]Hematology and Bone Marrow Transplant Unit, Ospedale Papa Giovanni XXIII, Bergamo, Italy. [5]Department of Hematology and Istituto L. and E. Seragnoli, University of Bologna, Bologna, Italy.

**Note:** Supplementary data for this article are available at Cancer Research Online (http://cancerres.aacrjournals.org/).

Current address for S.A. Mariani: The Queen's Medical Research Institute, Centre for Inflammation Research, The University of Edinburgh, Scotland, United Kingdom.

**Corresponding Author:** Bruno Calabretta, Thomas Jefferson University, 233 S. 10th Street, Philadelphia, PA 19107. Phone: 215-503-4522; E-mail: bruno.calabretta@jefferson.edu

**doi:** 10.1158/0008-5472.CAN-17-2644

Published OnlineFirst December 12, 2017; DOI: 10.1158/0008-5472.CAN-17-2644



and celastrol is a potent proteasome inhibitor that has pleiotropic effects including the inhibition of NF-κB (28, 29).

To overcome these limitations, we sought to identify MYB-dependent pathways that may be targeted therapeutically. We show here that cyclin D3, CDK6, and BCL2 are relevant MYB targets with essential roles for *in vitro* growth and leukemogenesis of $Ph^+$ ALL cells. These findings provide a "proof of concept" demonstration of how to exploit the TF "addiction" of leukemic cells.

## Materials and Methods

### Cell culture

BV173 (CML-lymphoid blast crisis cell line) were kindly provided by Dr. N. Donato (NIH), SUP-B15 ($Ph^+$ ALL cell line) were purchased from the ATCC, and Z181 ($Ph^+$ ALL cell line) were kindly provided by Dr. Z. Estrov (M.D. Anderson Cancer Center, Houston, TX). TKI-resistant BV173 cells were generated by step-wise selection in the presence of increasing concentrations of imatinib, which induced the outgrowth of cells with the BCR-ABL1 T315I mutation. Experiments were performed on cell lines cultured for less than 30 passages. Mycoplasma was tested monthly following an established procedure (30). Cell lines were routinely authenticated by monitoring B-cell markers and BCR-ABL1 isoform expression. Cell lines were cultured in Iscove's Medium (Gibco) supplemented with 10% FBS, 100 U/mL penicillin–streptomycin, and 2 mmol/L L-glutamine at 37°C. Primary human $Ph^+$ ALL cells were maintained in SFEM (Stem Cell Technology) supplemented with SCF (40 ng/mL), Flt3L (30 ng/mL), IL3 (10 ng/mL), IL6 (10 ng/mL), and IL7 (10 ng/mL; PeproTech). Information on primary $Ph^+$ ALL samples used in this study is shown in Supplementary Table S1.

### Cell proliferation, cell-cycle analysis, and colony formation assay

3-(4,5-dimethylthiazol-2-yl)-2,5-diphenyltetrazolium bromide (MTT) assay was performed in 96-multiwell plates. Cells were incubated with 0.5 mg/mL MTT (Sigma Aldrich) at 37°C for 2 hours; then, formazan crystals were dissolved with 0.1 mol/L HCl in 2-propanol and absorbance was measured at 570 nm. Cell-cycle analyses were performed by propidium iodide staining (50 μg/mL) of cells permeabilized with 0.1% Triton and 0.1% sodium citrate followed by flow cytometry determination of DNA content. For clonogenic assays, cells were pretreated with 1 μg/mL doxycycline (Research Product International) for 24 hours or treated with drugs and immediately seeded in 1% methylcellulose medium (Stem Cell Technology) at 2,500 to 5,000 cells/mL. Colonies were counted after 7 to 10 days.

### Immunoblot

Cells were counted and lysed at a density of 10,000/μL in Laemmli Buffer. Lysates where run on polyacrylamide gels (Biorad), transferred onto nitrocellulose membranes, and incubated with primary antibodies (described in Supplementary Methods) and horseradish peroxidase–conjugated secondary antibodies (Thermo Fisher Scientific). Images were obtained by chemiluminescent reaction and acquisition on autoradiography films (Denville Scientific). Different antibodies were probed on the same nitrocellulose membrane; if necessary, previous signals were removed by incubation in stripping buffer (62 mmol/L Tris-HCl, pH 6.8, 2% SDS, β-mercaptoethanol 0.7 %) for 20 minutes at 50°C or by incubation with 0.5% sodium azide for 10 minutes at room temperature.

### Quantitative reverse-transcription PCR

RNA was isolated with RNeasy Plus Mini Kit (Qiagen) and reverse-transcribed with the High-Capacity cDNA Reverse Transcription Kit (Thermo Fisher Scientific). A total of 10 ng of cDNA was used as template and amplified with Power SYBR-Green PCR Master Mix (Thermo Fisher Scientific). When possible, primers were designed to span exon–exon junctions and are listed in the Supplementary Methods section.

### Lentiviral/retroviral vectors

For MYB silencing, we used the MYB shRNA kindly provided by Dr. Tom Gonda (31). For silencing of p21 (the protein product of the *CDKN1A* gene), CDK4, and CDK6, the pLKO.1 plasmids constitutively expressing the shRNAs and conferring puromycin resistance were purchased from GE Dharmacon [pLKO.1-Scramble: Addgene #1864; p21 (CDKN1A) shRNA: GE Dharmacon #TRCN0000040125; CDK4 shRNA: GE Dharmacon #TRCN0000000363; CDK6 shRNA: GE Dharmacon #TRCN0000010081]. For exogenous expression of CDK6, the RNA extracted from BV173 cells was reverse transcribed, and the full-length cDNA corresponding to transcript variant 1 (NCBI: NM_001259.6) was PCR-amplified with a forward primer introducing the XbaI restriction site and a reverse primer introducing the BamHI site. Then the product was digested and inserted in the XbaI-BamHI sites of the lentiviral vector pUltra-hot developed by Dr. Malcolm Moore (Addgene plasmid # 24130), which expresses the cDNA of interest and the mCherry protein as a bi-cistronic transcript under the control of the ubiquitin C promoter. The cyclin D3 cDNA (NCBI: NM_001760.4) was similarly obtained by total RNA purified from BV173 cells and inserted in the XbaI-BamHI sites of the pUltra-chili lentiviral vector (Dr. Malcolm Moore; Addgene plasmid # 48687), which expresses dTomato as a reporter protein. To obtain a nucleus-localized CDK4 protein, *CDK4* (NM_000075.3) was PCR amplified from BV173 cDNA by using a forward primer introducing an XbaI site and a reverse primer introducing a BamHI site following a sequence encoding the nuclear localization signal from the SV40 large T antigen (CCAAAGAAGAAGCGTAAGGTA). The CDK4-NLS product was then inserted in the XbaI-BamHI sites of the pUltra-Hot vector. MYB cDNA was PCR amplified from the MigR1-MYB plasmid (32) and inserted into the XbaI-NheI sites of pUltra-hot. To obtain the shRNA-resistant MYB cDNA, the entire plasmid was amplified with primers harboring point mutations in the MYB sequence targeted by the shRNA, which were designed to preserve the integrity of the amino acid sequence of MYB. Then, the linear plasmid was self-ligated and sequenced to confirm that the expected mutations were introduced. The E308G mutation was introduced by a similar method. The pLXSP-BCL2 retrovirus was previously described (33). Lentiviral or retroviral VSV-G pseudotyped particles were produced by calcium phosphate transfection of plasmid vectors into HEK-293T cells in combination with helper plasmids. Twenty-four hours later, the supernatant was collected, 0.45 μm filtered, and used to transduce BV173 or SUP-B15 cells by spinoculation in the presence of 8 μg/mL polybrene (Sigma-Aldrich). Transduced cells were either FACS-purified on the basis of the fluorescent reporter protein or selected with 3 μg/mL puromycin (Sigma-Aldrich).

### Microarray analysis

MYB-shRNA SUP-B15 and BV173 cells were treated for 24 hours with doxycycline or left untreated. RNA was isolated by

Published OnlineFirst December 12, 2017; DOI: 10.1158/0008-5472.CAN-17-2644



using the RNeasy Plus Mini Kit (Qiagen). RNA was quantified on a Nanodrop ND-100 spectrophotometer, followed by RNA quality assessment by analysis on an Agilent 2200 TapeStation (Agilent Technologies). Fragmented, biotin-labeled cDNA was synthesized using the Affymetrix WT Plus Kit (Thermo Fisher Scientific) for BV173 cells or the Ovation PICO WTA-system V2 and cDNA biotin module (NuGen Technologies) for SUP-B15 cells. cDNA from BV173 cells was hybridized onto Affymetrix gene chips, and Human Clariom S assays (Thermo Fisher Scientific) and cDNA from SUP-B15 cells were hybridized onto Human Gene 1.0 ST Array (Thermo Fisher Scientific) following the manufacturer's instructions. Arrays were scanned on an Affymetrix Gene Chip Scanner 3000, using Command Console Software. Quality Control of the experiment was performed by Expression Console Software v1.4.1. Genes were considered differentially expressed when cDNA fold change was >1.5. Differentially expressed genes common to both datasets were used for pathway analysis using IPA software. Microarray data obtained in this study have been deposited in NCBI Gene Expression Omnibus under GEO Series accession number GSE105826.

### Immunofluorescence

Cells were cytospun on polylysine-coated glass slides, fixed with 3.7% formaldehyde, permeabilized with Triton 0.1%, and incubated overnight at 4°C with primary antibodies anti-CDK4 or anti-CDK6 followed by Alexa Fluor 594–conjugated anti-rabbit or anti-mouse secondary antibodies (Thermo Fisher Scientific, 1 hour at room temperature) and then mounted with DAPI-Fluoromount G (Southern Biotech #0100-20). Imaging was acquired with a Nikon Eclipse Ti C2 laser confocal microscope with objective Plan Apo 60X/1.40 oil and processed with NIS Elements AR 4.5 software.

### Chromatin immunoprecipitation

BV173 and SUP-B15 cells were processed with the SimpleChIP Enzymatic Chromatin IP Kit (Cell Signaling Technology; #9002) following the manufacturer's instruction. Chromatin from $4 \times 10^6$ cells was used for each immunoprecipitation with specific primary antibodies or equal amounts of normal rabbit immunoglobulins. The purified DNA segments were quantified by qPCR and normalized to the amount of input material.

### Animals

Ph$^+$ ALL cells ($2 \times 10^6$ cells/mouse) were injected intravenously in 6- to 8-week-old NOD/SCID-IL-2Rγ–null mice (Jackson Laboratory). Doxycycline was administered at 2 g/L in the drinking water starting 7 days after injection. Peripheral blood leukemic cells were monitored by flow cytometry detection of GFP, human CD10, and/or CD19 (based on cell type–specific expression). For immunoblot analysis, leukemic cells were purified from murine cells by FACS or with the EasySep Mouse/Human Chimera Isolation Kit (StemCell Technologies). Palbociclib (obtained by Pfizer) was dissolved at 15 mg/mL in 50 mmol/L sodium lactate, pH = 4.0, and given by oral gavage for 10 consecutive days at 150 mg/kg. Sabutoclax (SelleckChem) was dissolved at 0.5 mg/mL in 10:10:80 Kolliphor-EL (Sigma-Aldrich)-ethanol-PBS and administered intraperitoneally every other day at 5 mg/kg for a total of five doses. Animal experiments were approved by the Institutional Animal Care and Use Committee of Thomas Jefferson University under protocol number 00012.

### Statistical analysis

Results are expressed as mean ± SEM. Statistical significance was determined by unpaired two-tailed Student *t* test. Bonferroni correction was applied in cases of multiple comparisons. Correlation studies were analyzed by the Pearson test, and significance was calculated by the Student *t* distribution. Significance in survival experiment was assessed by the log-rank test. For drug combination studies, the combination index (CI) was calculated by the Chou–Talalay method (34), and synergism was defined as CI < 1.

## Results

### MYB silencing suppresses Ph$^+$ ALL cell growth

We showed previously that loss of a *Myb* allele impairs colony formation of p190-BCR-ABL1–transformed B-cell progenitors and suppresses B-cell leukemia in mice, but has no effect on normal B-cell development (15).

To investigate if MYB is similarly required in Ph$^+$ ALL, we assessed the effects of MYB silencing in human cell lines BV173, SUP-B15, and Z181 transduced with the doxycycline (DOX)-inducible, GFP-expressing pLVTSH-MYB shRNA lentiviral vector (31). DOX treatment abolished MYB expression in the three cell lines (Fig. 1A; Supplementary Fig. S1A and S1B). Compared with controls, DOX-treated BV173 cells exhibited (i) cell-cycle arrest in the $G_0$–$G_1$ phase (Fig. 1B); (ii) growth inhibition revealed by MTT assays (Fig. 1C); and (iii) reduced colony formation (Fig. 1D). These effects were also observed in SUP-B15 and Z181 cells (Supplementary Fig. S1C–S1F). These findings were not due to off-target effects, because expression of an MYB cDNA carrying synonymous point mutations on the shRNA target sequence (Supplementary Fig. S2A–S2C) rescued the impaired proliferation and colony formation of MYB-silenced BV173 cells (Supplementary Fig. S2D and S2E). The effects of MYB silencing were also tested in TKI-resistant T315I BV173 cells; as shown in Fig. 1E–H, growth suppression induced by DOX treatment was undistinguishable from that in parental BV173 cells. As expected, treatment with imatinib or dasatinib markedly suppressed colony formation of parental BV173 cells but had no effect on the TKI-resistant derivative line (compare Fig. 1D and H).

### MYB silencing suppresses leukemia development in NOD/SCID-IL-2Rγ–null mice

Then, we assessed the requirement of MYB for leukemia development in NOD/SCID-IL-2Rγ–null (NSG) mice (35) injected with BV173 cells and treated with DOX. Six weeks after cell injection, DOX treatment induced a dramatic decrease of leukemia burden revealed by flow cytometry and cytokine-independent colony formation of bone marrow BV173 cells (Fig. 2A and B).

Mice injected with shMYB BV173 cells were also monitored for survival. Untreated mice died of leukemia (bone marrow heavily infiltrated by leukemic cells and splenomegaly) within 8 weeks (average survival = 42 days); mice given DOX to induce MYB silencing survived up to 200 days with no signs of disease, except for one animal whose cause of death could not be determined (Fig. 2C). All mice were sacrificed at the 200th-day endpoint, and flow cytometry of bone marrow cells revealed no leukemic cells (Supplementary Fig. S3A), indicating that MYB silencing markedly suppressed or eradicated the disease. As expected, ectopic

Published OnlineFirst December 12, 2017; DOI: 10.1158/0008-5472.CAN-17-2644



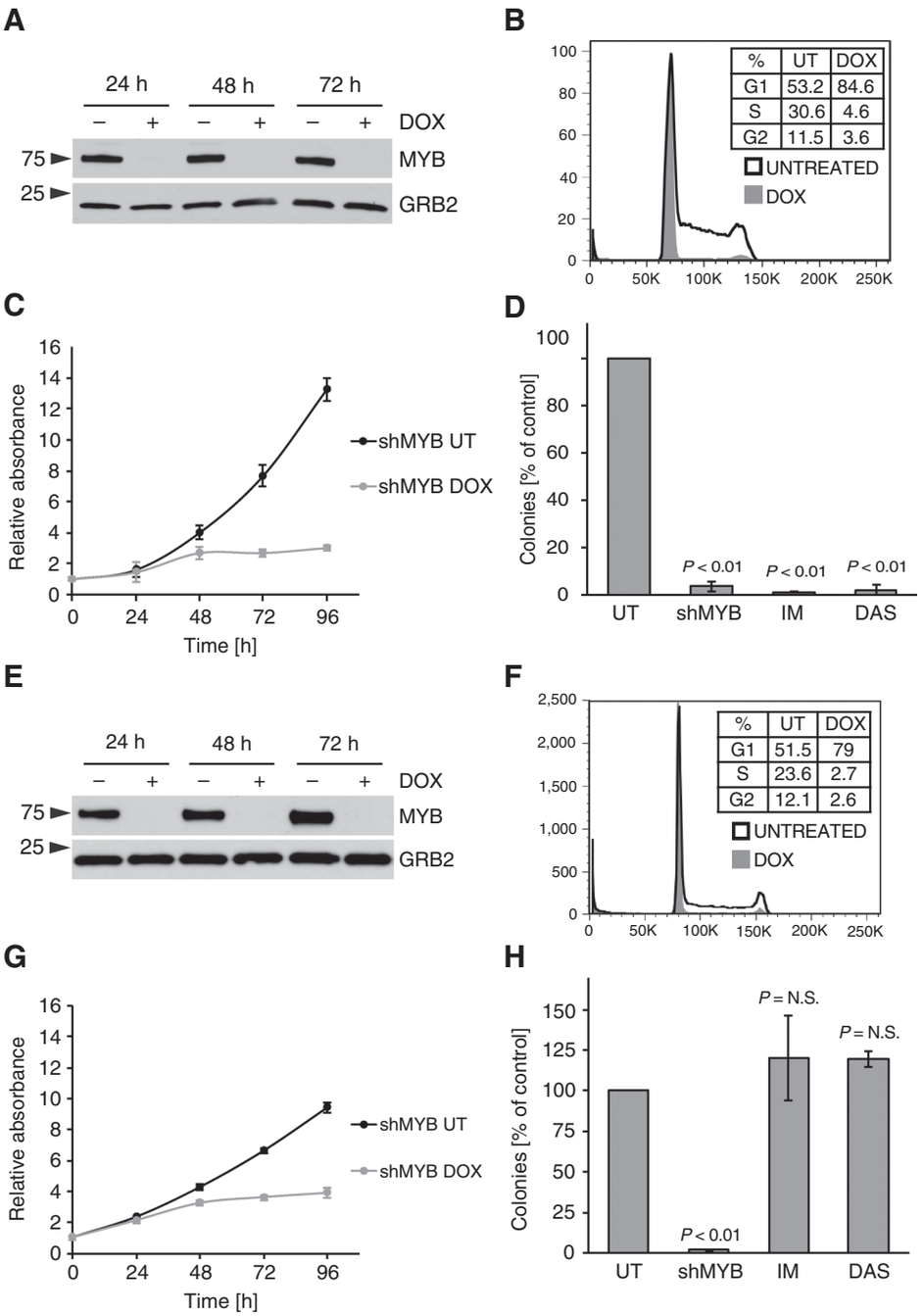


**Figure 1.**
MYB silencing reduces viability and proliferation of Ph$^+$ ALL BV173 cell line and of its TKI-resistant (T315I) derivative. **A–C,** immunoblot (**A**), cell-cycle analysis at 48 hours of treatment (**B**), and cell growth at the indicated times (**C**) of untreated or DOX-treated BV173 shMYB cells. **D,** methylcellulose colony formation assay of BV173 shMYB cells untreated, treated with DOX to induce MYB silencing (shMYB), imatinib (IM) 1 μmol/L, or dasatinib (DAS) 2 nmol/L. **E–H**, Experiments performed as in **A–D** on the TKI-resistant cell line T315I BV173 shMYB. N.S., nonsignificant.

expression of shRNA-resistant MYB rescued the leukemogenesis of shMYB BV173 cells (Fig. 2C).

DOX treatment also induced a marked increase in the survival of NSG mice injected with shMYB SUP-B15 cells. Control mice survived 53.0 ± 2.2 days; by contrast, one DOX-treated mouse died 115 days after cell injection with no obvious signs of disease (<10% circulating leukemic cells and no evidence of splenomegaly), and remaining mice were sacrificed, when moribund, 139 to 163 days after injection (Supplementary Fig. S3B). Interestingly, MYB expression was not silenced in bone marrow or spleen leukemia cell lysates from two terminally ill DOX-treated mice, whereas one sample displayed a shorter MYB isoform that may lack the shRNA target sequence (Supplementary Fig. S3C), likely explaining leukemia development in these animals. As control, MYB levels were markedly reduced in leukemic cells from a mouse injected with shMYB SUP-B15 cells and DOX-treated for 4 days, when peripheral blood GFP$^+$ cells were >50% (Supplementary Fig. S3C, lane 6).

We also investigated the requirement of MYB in NSG mice injected with shMYB-transduced patient-derived Ph$^+$ ALL cells (ALL-674). For this experiment, transduced cells (approximately 10% GFP-positive) were expanded in a recipient NSG mouse,

Published OnlineFirst December 12, 2017; DOI: 10.1158/0008-5472.CAN-17-2644



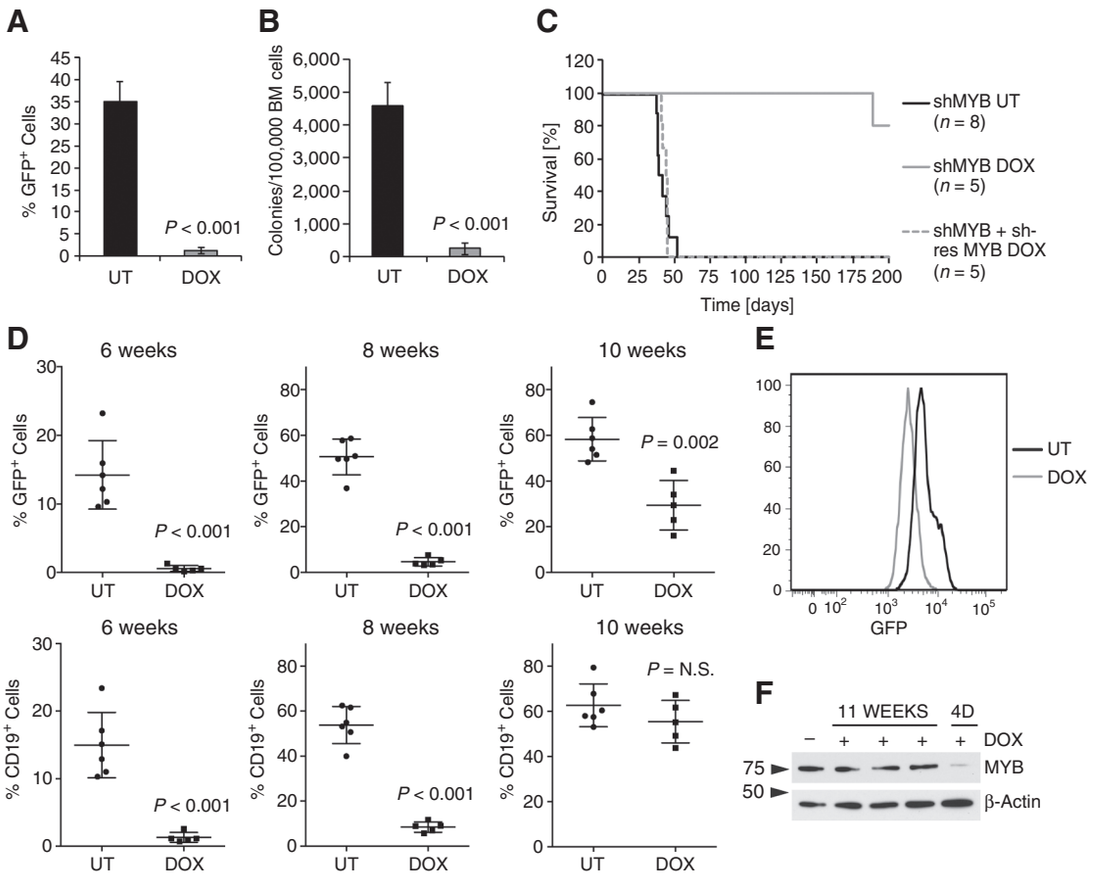


**Figure 2.**

MYB silencing suppresses leukemogenesis of Ph+ ALL cells in immunodeficient mice. **A** and **B,** Leukemia burden in untreated or DOX-treated NSG mice ($n = 4$) injected with BV173 shMYB cells assessed by flow cytometry analysis of GFP-positive bone marrow cells (**A**) or methylcellulose colony formation assay (**B**). **C,** Kaplan–Meier survival plot of untreated or DOX-treated NSG mice injected with BV173 shMYB cells or with BV173 shMYB cells expressing a shMYB-resistant form of MYB. **D,** Peripheral blood leukemia burden (percentage of GFP+ or CD19+ cells) in untreated ($n = 6$) or DOX-treated ($n = 5$) NSG mice injected with primary Ph+ ALL (#674) cells transduced with the shMYB lentivirus. **E,** Flow cytometry analysis of GFP positivity in the bone marrow of terminally ill untreated or DOX-treated NSG mice injected with ALL-674 shMYB cells (gated to exclude GFP-negative cells, plots display results from one representative untreated and one DOX-treated mouse). **F,** Immunoblot of MYB expression in GFP-sorted bone marrow cells from NSG mice injected with ALL-674 shMYB cells and continuously treated with DOX for 11 weeks (lanes 2–4) or after a four-day (4D) treatment initiated when peripheral blood GFP-positive cells were >50% (10 weeks after injection). N.S., nonsignificant.

GFP-sorted from the bone marrow and injected in female NSG recipient mice to obtain a more efficient engraftment (33). Leukemia progression was monitored by periodic analysis of total leukemic (CD19+) or shMYB-transduced (GFP+) cells. At 6 weeks, DOX-treated mice showed reduced numbers of CD19+ or GFP+ cells compared with untreated mice; however, by 10 weeks, we observed an outgrowth of leukemic cells, a fraction of which was GFP-negative (Fig. 2D). In addition, among GFP+ cells, average GFP intensity was reduced (Fig. 2E) and MYB expression was not downregulated (Fig. 2F), suggesting selection of leukemic cells expressing low levels of the MYB shRNA.

### MYB modulates the expression of cell-cycle–regulatory genes

To investigate mechanisms responsible for the "MYB dependence" of Ph+ ALL cells, we performed microarray analysis of MYB-silenced SUP-B15 and BV173 cells. Seventy-nine genes were differentially expressed in both cell lines (Fig. 3A). Ingenuity pathway analysis revealed that cell-cycle progression, DNA replication, and cell-cycle checkpoints were the pathways most significantly affected by MYB silencing. In addition, BCL2 was also significantly downregulated (Fig. 3A). qPCR analysis confirmed the downregulation of *CDK6*, *cyclin D3* (*CCND3*), *CDK2*, *cyclin E2* (*CCNE2*), and *FOXM1* and the upregulation of the CDK inhibitor *p21* (*CDKN1A*; Fig. 3B; Supplementary Fig. S4A). Immunoblots of MYB-silenced BV173 and SUP-B15 cells confirmed the increase in p21 expression and the downregulation of CDK6 and cyclin D3 (Fig. 3C and D); these changes were associated with markedly reduced CDK4/6-dependent RB phosphorylation (36, 37) and expression of FOXM1 (Fig. 3C and D), a CDK4/6 substrate stabilized through phosphorylation (38). Expression of RB was partially reduced in MYB-silenced cells; instead, levels of p130-RBL2 were increased and the protein migrated faster than in untreated cells consistent with loss of phosphorylation (Fig. 3C and D). These changes were confirmed in MYB-silenced ALL-674 cells purified from the bone marrow of two DOX-treated (4 days) mice (Fig. 3E). By chromatin immunoprecipitation (ChIP) in

Published OnlineFirst December 12, 2017; DOI: 10.1158/0008-5472.CAN-17-2644



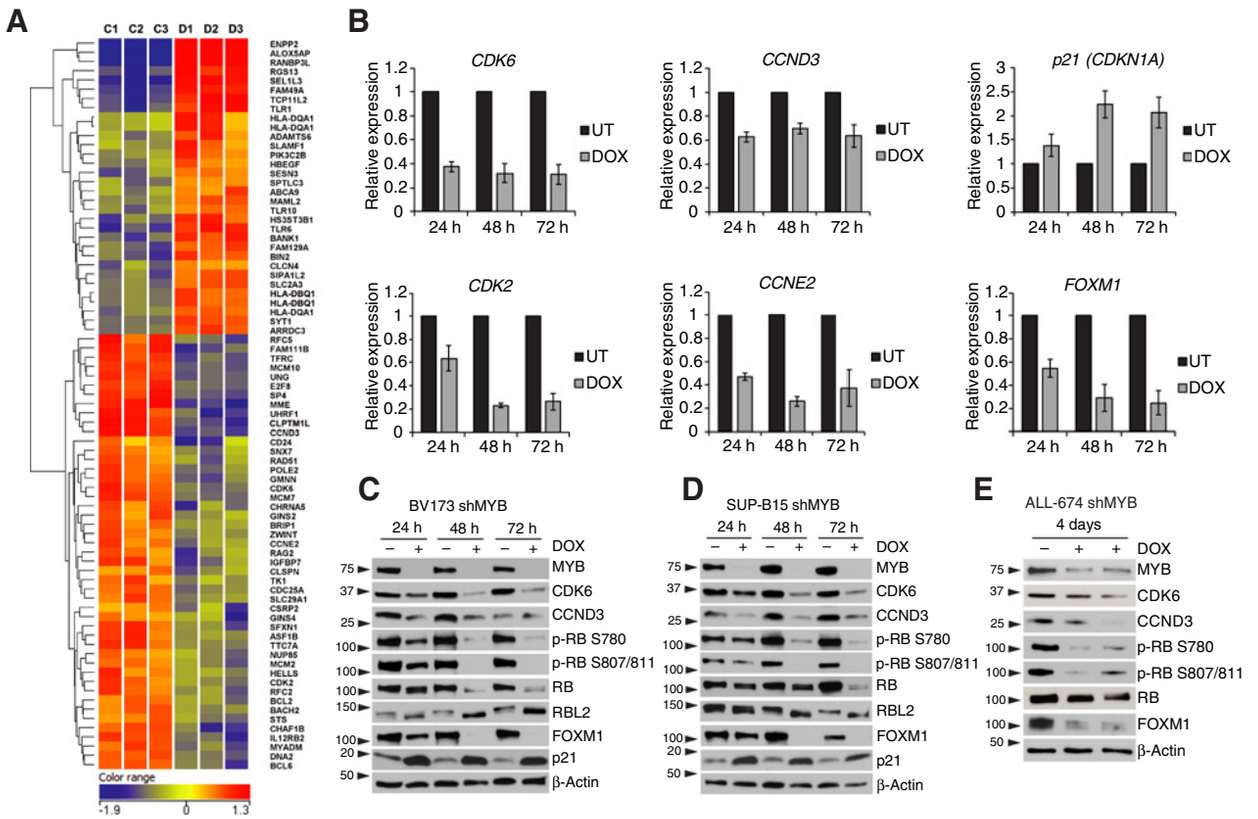


**Figure 3.**

MYB silencing alters the expression of cell-cycle–regulatory genes. **A,** Heatmap of 79 genes significantly modulated in BV173 shMYB and SUP-B15 shMYB cell lines (C1, C2, and C3 denote untreated controls; D1, D2, and D3 denote samples treated with DOX for 24 hours). **B,** qPCR analysis of *CDK6, cyclin D3* (*CCND3*), *p21 (CDKN1A), CDK2, cyclin E2* (*CCNE2*), and *p21* (*CDKN1A*) expression in BV173 shMYB cells untreated or DOX-treated for the indicated time points (normalized to GAPDH). **C–E,** Immunoblot analysis of cell-cycle–regulatory genes in MYB-silenced Ph$^+$ cell lines (**C** and **D**) or ALL-674 shMYB cells DOX-treated for 4 days *in vivo* and GFP-sorted (**E**).

BV173 (Fig. 4A–C) and SUP-B15 cells (Supplementary Fig. S4B), we detected binding of MYB to the promoter of the *CDKN1A* and *CCND3* genes and to the promoter and intron 5 enhancer of the *CDK6* gene (39). These regions contain putative MYB-binding sites, suggesting that CDK6, cyclin D3, and p21 expression is directly regulated by MYB. As a positive control, MYB was detected at the promoter of the *BCL2* gene in BV173 and SUP-B15 cells (Supplementary Fig. S4C). To further investigate the significance of these findings, mRNA levels of MYB and its putative targets were analyzed in 24 primary human Ph$^+$ ALL samples. We observed a strikingly positive correlation between *MYB* and *CDK6* expressions ($P = 0.00008$), whereas that between MYB and cyclin D3 or p21 was not significant after Bonferroni correction (Fig. 4D–F). A positive correlation between *MYB* and *CDK6* expressions was also noted in 226 samples of adult B-cell ALL (Fig. 4G; ref. 40), in 207 samples of Ph-negative, high-risk childhood ALL (Fig. 4H; ref. 41), and in 174 AML samples from The Cancer Genome Atlas (Fig. 4I).

### CDK6 but not CDK4 expression is necessary for Ph$^+$ ALL cell proliferation

In MYB-silenced BV173 and SUP-B15 cells, expression of CDK6 is markedly downregulated while levels of CDK4 are not affected (Fig. 5A and B). Because CDK4 and CDK6 should have redundant roles in $G_1$–S phase transition and CDK4 is expressed in most cases of Ph$^+$ ALL (Fig. 5C), we asked whether decreased CDK6 levels can explain the cell-cycle arrest of MYB-silenced cells. Thus, BV173 and SUP-B15 cells were transduced with CDK4 or CDK6 shRNAs. Surprisingly, CDK4 silencing had negligible effects, whereas CDK6 silencing suppressed cell-cycle progression, RB phosphorylation, and FOXM1 expression in both lines (Fig. 5D–G). These data suggest that in Ph$^+$ ALL cells, CDK6 exerts a function that is not shared by CDK4. Interestingly, confocal microscopy analysis revealed that CDK6 is predominantly localized in the nucleus of Ph$^+$ ALL cells, whereas CDK4 is almost exclusively cytoplasmic (Fig. 5H). To investigate whether the cytoplasmic localization of CDK4 may explain its inability to rescue the growth suppression induced by CDK6 silencing, a nucleus-localized form of CDK4 (CDK4-NLS) was expressed in BV173 shMYB cells transduced with a lentiviral vector expressing cyclin D3 (because the latter is also downregulated in MYB-silenced cells). In cells expressing cyclin D3 alone, CDK4 was predominantly cytoplasmic; by contrast, CDK4 was mostly nuclear in cells expressing CDK4-NLS (Supplementary Fig. S5A). Upon DOX treatment to silence MYB expression, coexpression of cyclin D3 and CDK4-NLS partially restored RB phosphorylation and FOXM1 expression (Supplementary Fig. S5B) and resulted in a significant increase in the percentage of proliferating cells

Published OnlineFirst December 12, 2017; DOI: 10.1158/0008-5472.CAN-17-2644



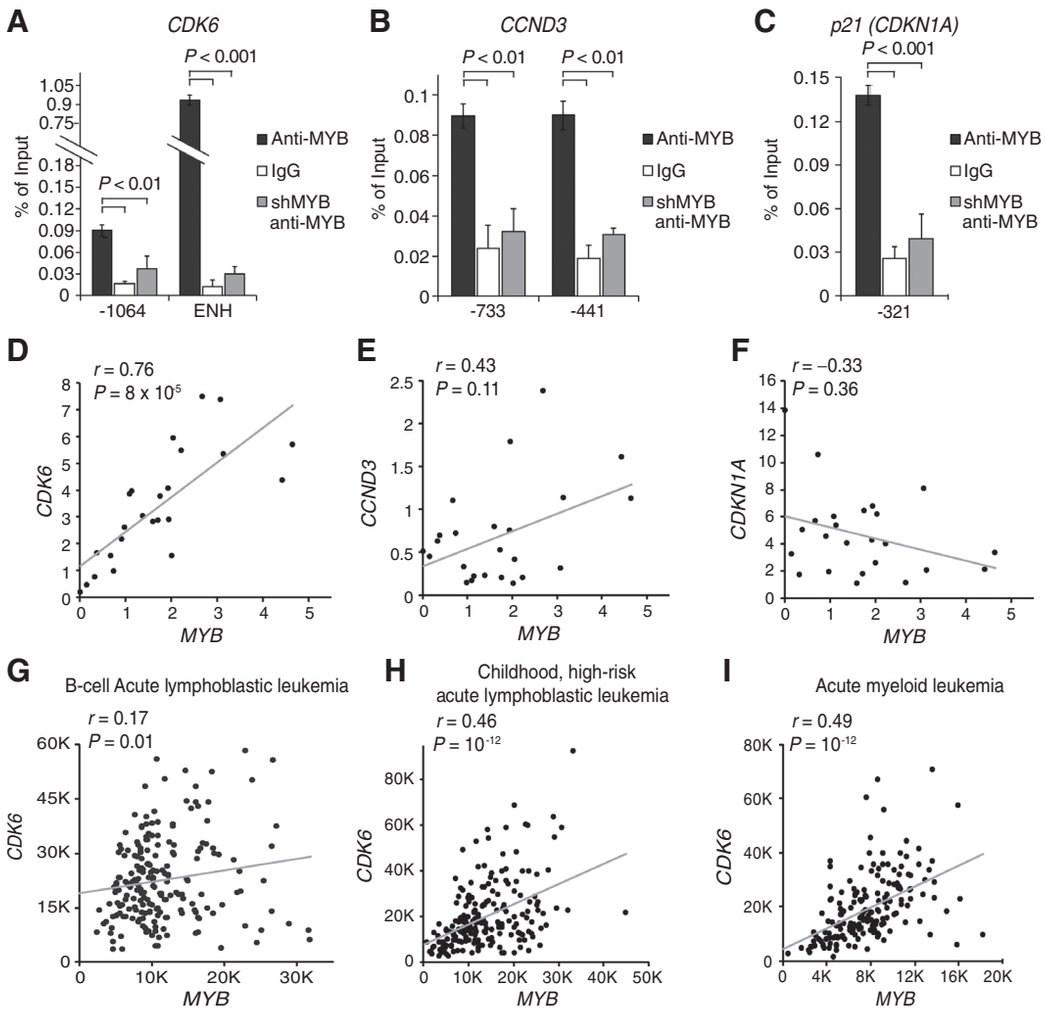


**Figure 4.**

MYB regulates the expression of cell-cycle–regulatory genes and is coexpressed with CDK6 in different types of leukemia. **A–C,** MYB binding by ChIP to regulatory regions of the *CDK6* (**A**), *CCND3* (**B**), or *CDKN1A* (**C**) genes in BV173 cells (numbers refer to the position of the forward primer relative to the TSS). As negative controls, ChIPs were performed with a nontargeting antibody (white bars) or with an anti-MYB antibody on lysates from MYB-silenced BV173 cells (gray bars). **D–F,** Plot of the correlation between the mRNA levels (by qPCR) of *MYB* and *CDK6* (**D**), *MYB* and *CCND3* (**E**), or *MYB* and *CDKN1A* (**F**) in 24 samples of primary human Ph$^+$ ALL samples. **G,** Plot of the correlation between the expression (by microarray) of *MYB* and *CDK6* in a panel of 226 B-cell ALL of mixed cytogenetics (GSE79533). **H,** Plot of the correlation between the expression (by microarray) of *MYB* and *CDK6* in a panel of 207 Ph-negative childhood, high-risk ALL (GSE11877). **I,** Plot of the correlation between the expression of *MYB* and *CDK6* based on The Cancer Genome Atlas data on 174 samples of AML of mixed cytogenetics (RNA-seq, median expression).

(Supplementary Fig. S5C) compared with empty vector (EV)–transduced cells.

### Restoring expression of CDK6, cyclin D3, and BCL2 rescues cell-cycle arrest and apoptosis induced by MYB silencing

Next, we asked whether restoring the expression of cyclin D3 and CDK6 would be sufficient to rescue the proliferative arrest of MYB-silenced cells.

Expression of CDK6 alone partially restored RB phosphorylation and rescued FOXM1 expression, whereas expression of cyclin D3 alone did not (Supplementary Fig. S6A). CDK6 expression partially rescued the reduced growth of MYB-silenced cells, whereas cyclin D3 expression had a modest effect (Supplementary Fig. S6B).

Coexpression of CDK6 and cyclin D3 (K6/D3) restored RB phosphorylation and FOXM1, *CDK2*, and cyclin E2 (*CCNE2*) expression (Fig. 6A–C), and rescued the cell-cycle arrest of cells treated with DOX for 2 days (Fig. 6D and E). However, MYB-silenced K6/D3 cells grew less vigorously after 4 days of DOX treatment (Fig. 6F) and did not form colonies in methylcellulose (Fig. 6G).

Based on these findings, we asked whether induction of apoptosis could explain the reduced growth of MYB-silenced K6/D3 BV173 cells. Indeed, although sub-$G_1$ apoptotic cells were not detected by cell-cycle analysis of shMYB BV173 or SUP-B15 cells performed after 2 days of DOX treatment (Fig. 1B and F, Fig. 6D and E; Supplementary Fig. S1B), a 4-day DOX treatment increased the percentage of Annexin V$^+$ cells and induced caspase 3 cleavage in EV and K6/D3 cells (Fig. 6H and I).

Published OnlineFirst December 12, 2017; DOI: 10.1158/0008-5472.CAN-17-2644



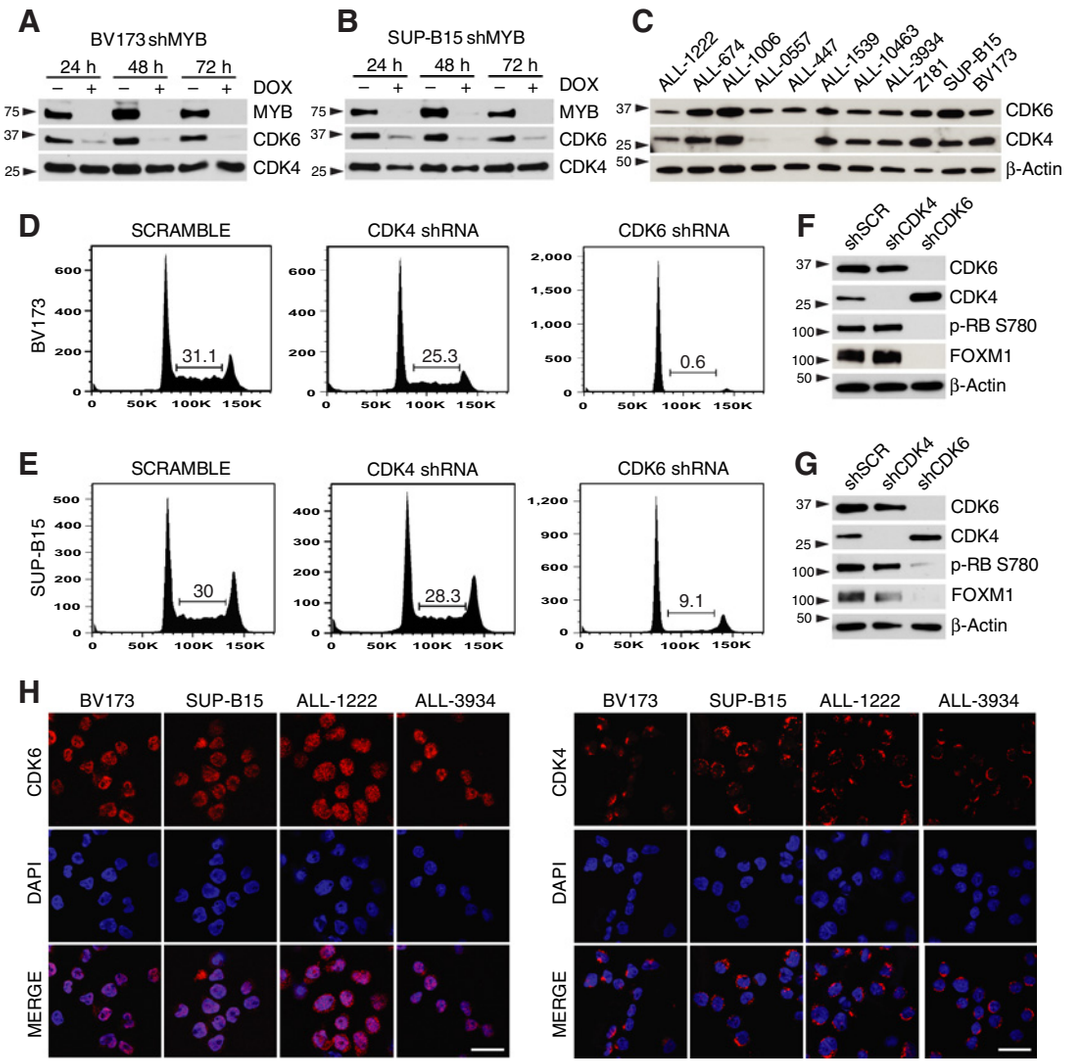


**Figure 5.**

Expression of CDK6 but not CDK4 is required for the proliferation of $Ph^+$ ALL cells. **A–C,** Immunoblot of CDK6 and CDK4 expression in untreated or DOX-treated BV173 shMYB cells (**A**) or SUP-B15 shMYB cells (**B**) and in untreated primary $Ph^+$ ALL cells (**C**). **D** and **E,** Representative experiment showing the cell-cycle analysis of scramble, CDK4, or CDK6 constitutive shRNA-transduced BV173 (**D**) or SUP-B15 (**E**) cells. Compared with scramble-transduced cells, the decrease in the percentage of S phase cells is significant in BV173 shCDK6 cells ($P = 10^{-5}$) and in SUP-B15 shCDK6 cells ($P = 0.001$), but not in BV173 shCDK4 or SUP-B15 shCDK4 cells (results are from three independent experiments). **F** and **G,** Immunoblot analysis of CDK4, CDK6, RB phosphorylation, and FOXM1 expression in scramble, CDK4, or CDK6 shRNA–transduced BV173 (**F**) or SUP-B15 (**G**) cells. **H,** Subcellular localization of CDK6 (left panels) or CDK4 (right panels) in BV173, SUP-B15, and primary human $Ph^+$ ALL cells (ALL-1222 and ALL-3934) by immunofluorescence-confocal microscopy (scale bar, 20 μm).

BCL2 was previously reported to be a MYB target (42–45), and thus, its decreased expression may contribute to the apoptosis of MYB-silenced cells (Fig. 6J and K). To test this hypothesis, we generated a derivative shMYB BV173 K6/D3 cell line named KDB in which levels of ectopically expressed BCL2 were not affected by MYB silencing (Fig. 6L). In these cells, BCL2 expression inhibited apoptosis, restored cell growth, and partially rescued the loss of colony formation induced by MYB silencing (Fig. 6M–O).

The defective colony formation potential of MYB-silenced KDB cells was not caused by increased p21 expression because silencing p21 did not further increase colony formation of DOX-treated KDB cells (Supplementary Fig. S6C–S6F).

Finally, we tested whether these derivative lines induce leukemia in NSG mice. Mice injected with shMYB BV173 cells expressing K6/D3 or BCL2 alone and given DOX did not develop leukemia. However, 10 of 12 DOX-treated mice injected with KDB or KDBp cells developed leukemia, and 9 of them succumbed to the disease by 200 days (Fig. 6P).

### The recruitment of p300/CBP is required for MYB-dependent control of proliferation but is dispensable for its antiapoptotic effects

The interaction between MYB and the histone acetyltransferases p300/CBP is critically important for MYB function in hematopoietic cells (46–48). To assess the importance of p300/CBP

Published OnlineFirst December 12, 2017; DOI: 10.1158/0008-5472.CAN-17-2644



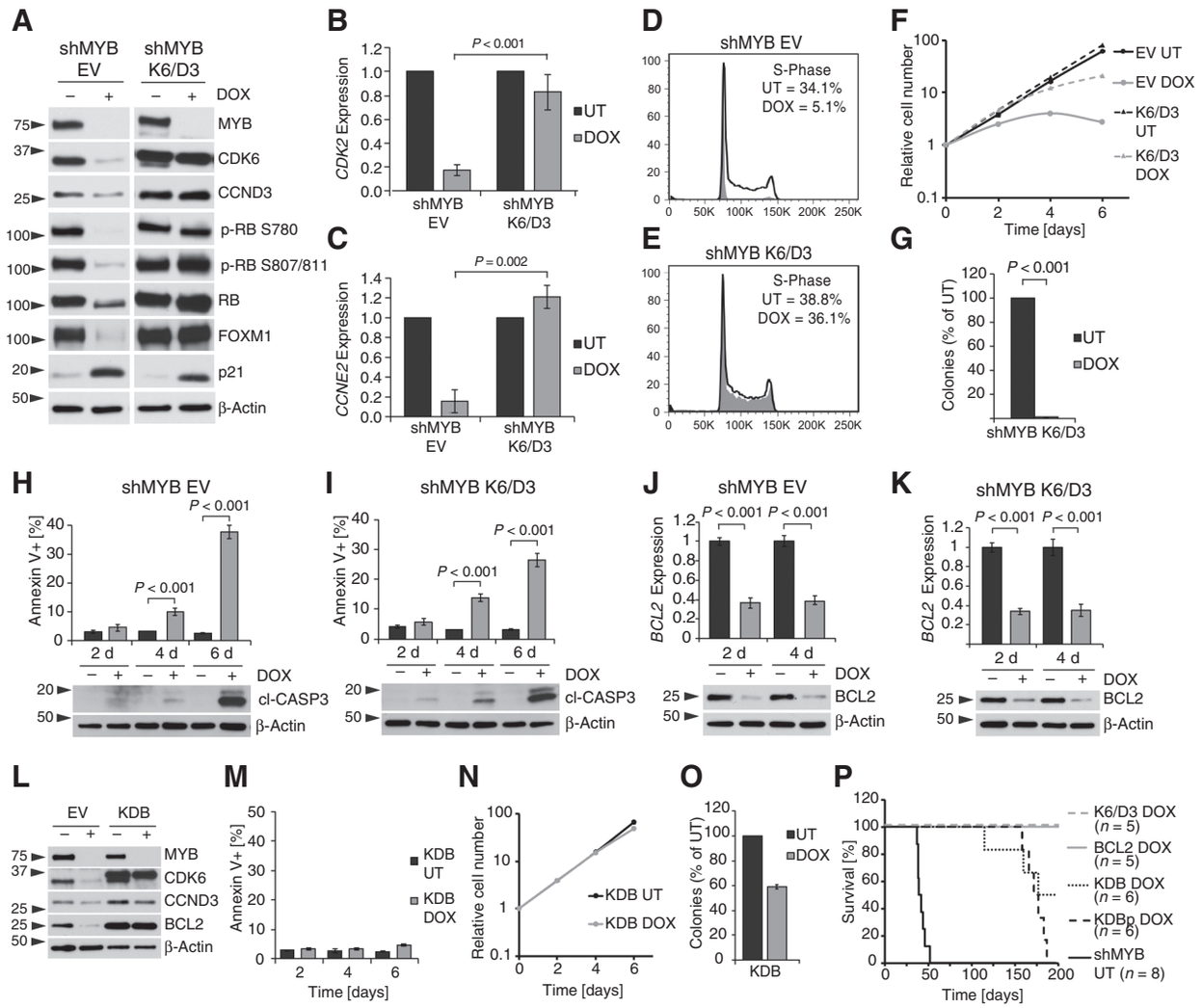


**Figure 6.**

Coexpression of CDK6/Cyclin D3 and BCL2 partially rescues the effects of MYB silencing. **A,** Immunoblot for MYB and its targets in untreated or DOX-treated (96 hours) BV173 shMYB EV or BV173 shMYB K6/D3 cells. **B** and **C,** qPCR for *CDK2* (**B**) and *cyclin E2* (**C**) in untreated or DOX-treated (48 hours) BV173 shMYB EV cells or BV173 shMYB K6/D3 cells. **D** and **E,** Cell-cycle analysis of untreated or DOX-treated (48 hours) BV173 shMYB EV (**D**) or BV173 shMYB K6/D3 (**E**) cells. **F,** Cell growth by MTT assay of untreated or DOX-treated BV173 shMYB EV cells or BV173 shMYB K6/D3 cells (vertical axis is shown as a logarithmic scale). **G,** Colony assay of untreated or DOX-treated BV173 shMYB K6/D3 cells. **H** and **I,** Annexin V positivity (top) and expression of cleaved caspase-3 by immunoblot (bottom) in untreated or DOX-treated (2, 4, or 6 days) BV173 shMYB EV (**H**) and BV173 shMYB K6/D3 (**I**) cells. **J** and **K,** qPCR for *BCL2* (top) and immunoblot for BCL2 (bottom) in untreated or DOX-treated (2 or 4 days) BV173 shMYB EV (**J**) or BV173 shMYB K6/D3 (**K**) cells. **L,** Immunoblot of EV and KDB derivative BV173 shMYB cell lines untreated or treated with DOX for 4 days. **M–O,** Annexin V positivity (**M**), cell growth by MTT assay (**N**; vertical axis is shown as a logarithmic scale), and methylcellulose colony formation assay (**O**) of untreated or DOX-treated KDB cells. **P,** Kaplan–Meier survival plot of NSG mice injected with untreated BV173 shMYB or DOX-treated BV173 shMYB derivative cell lines.

recruitment for MYB transcriptional effects, shMYB BV173 cells were transduced with the EV, the shRNA-resistant wild-type (WT) MYB, or the shRNA-resistant MYB-E308G mutant that does not interact with p300/CBP (48) and were treated with DOX to silence endogenous MYB.

Although expression of shRNA-resistant MYB WT completely rescued the effects of MYB silencing, DOX-treated MYB-E308G–expressing cells displayed decreased S phase and colony formation but no increase in Annexin V positivity (Supplementary Fig. S7A–S7C). By immunoblot analysis, expression of MYB-E308G rescued levels of BCL2 but not CDK6 and FOXM1 or RB phosphorylation (Supplementary Fig. S7D). To investigate mechanisms that may explain the differential requirement of p300/CBP in the regulation of CDK6 and BCL2, ChIP experiments were performed at the regulatory regions of these genes.

DOX-treated EV-transduced cells showed reduced levels of MYB and p300 binding and H3K27 acetylation at the promoter and enhancer of *CDK6* and at the promoter of *BCL2*, compared with cells expressing MYB-WT. MYB-E308G–expressing cells also showed reduced p300 binding and H3K27 acetylation at the promoter and enhancer of *CDK6*, but H3K27 acetylation was

Published OnlineFirst December 12, 2017; DOI: 10.1158/0008-5472.CAN-17-2644



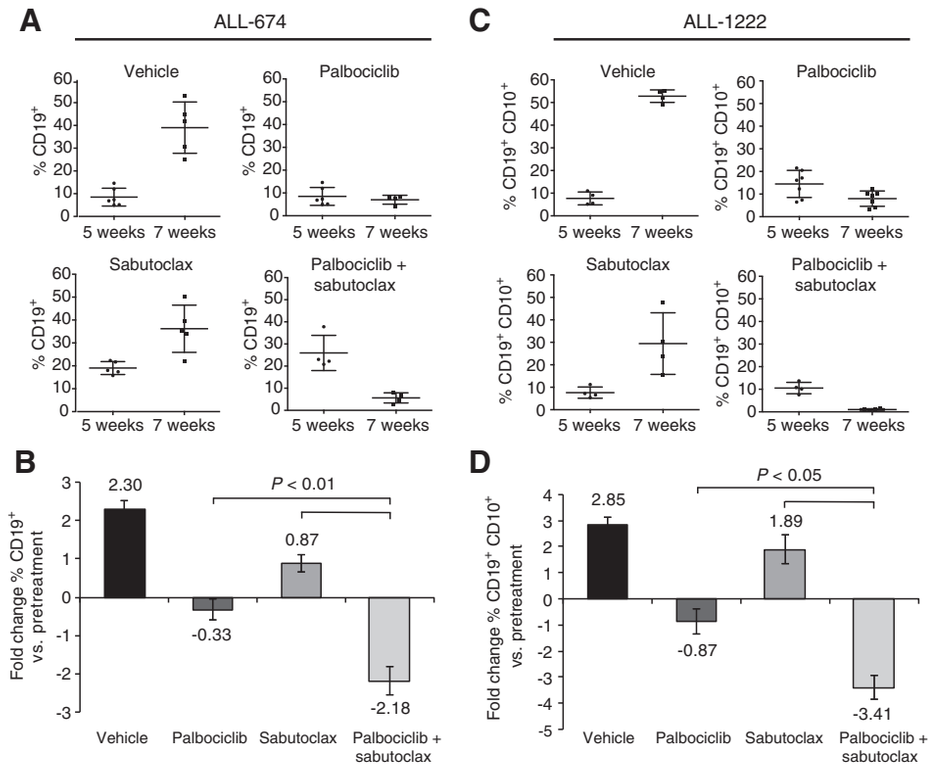


**Figure 7.**

Sabutoclax and palbociclib cooperate to suppress Ph$^+$ ALL in NSG mice. **A** and **B,** Percentage of CD19$^+$ cells in the peripheral blood (**A**) and fold changes in leukemia burden (**B**) of untreated and drug-treated NSG mice injected with sample ALL-674 before (5 weeks after injection) and after treatment (7 weeks after injection). **C** and **D,** Percentage of CD19$^+$CD10$^+$ cells in the peripheral blood (**C**) and fold changes in leukemia burden (**D**) of untreated and drug-treated NSG mice injected with sample ALL-1222 before (5 weeks after injection) and after treatment (7 weeks after injection); palbociclib was given by oral gavage for 10 consecutive days at 150 mg/kg, whereas sabutoclax was administered intraperitoneally every other day (five doses, 5 mg/kg).

not reduced at the *BCL2* promoter, in spite of lower p300 binding (Supplementary Fig. S7E–S7G).

### Cotreatment with the CDK4/6 inhibitor palbociclib and a BCL2 antagonist inhibits growth of Ph$^+$ ALL cells *ex vivo* and suppresses leukemia burden in NSG mice

Based on their essential role in cell growth, CDK6 and BCL2 might serve as targets to exploit the MYB "addiction" of Ph$^+$ ALL cells. First, we investigated the effects of the CDK4/CDK6 inhibitor palbociclib in primary Ph$^+$ ALL cells. Similar to its effects in cell lines (49), palbociclib inhibited the S phase of Ph$^+$ ALL cells (Supplementary Fig. S8A). Moreover, it suppressed colony formation of primary Ph$^+$ ALL cells, whereas normal CD34$^+$ cells were less affected (Supplementary Fig. S8B). Then, we assessed the effect of palbociclib in NSG mice injected with three different Ph$^+$ ALL samples. Compared with vehicle-treated mice, drug-treated animals displayed lower numbers of peripheral blood CD19$^+$ leukemia cells 6 to 8 weeks after cell injection (Supplementary Fig. S8C). However, the effect was transient, probably reflecting the cytostatic effects of palbociclib and/or the insufficient length of the treatment.

To mimic more faithfully the effects of MYB silencing, we used palbociclib in combination with the BCL2 antagonist venetoclax (50). The palbociclib/venetoclax combination had synergistic effects in BV173 and additive effects in SUP-B15 cells (Supplementary Fig. S9A–S9D). SUP-B15 cells were markedly more sensitive to venetoclax than BV173 cells (Supplementary Fig. S9E and S9F), likely because of lower MCL1 and BCL-XL and higher BIM expression (Supplementary Fig. S9G). Primary Ph$^+$ ALL cells display low proliferation *in vitro*, preventing analysis of the effects induced by the palbociclib/venetoclax combination. However, treatment with venetoclax induced apoptosis in three Ph$^+$ ALL samples, albeit at different drug concentrations (Supplementary Fig. S9H–S9J). In particular, sample #1006 was resistant to treatment with venetoclax, most likely because of much higher BCL-XL and MCL1 levels than in the other samples (Supplementary Fig. S9K).

Due to the sample-to-sample variability in expression of BCL2 family members and sensitivity to venetoclax, we tested the effects of the pan-BCL2 inhibitor sabutoclax (51). Treatment with the palbociclib/sabutoclax combination synergistically reduced the number of BV173 and SUP-B15 cells at most doses (Supplementary Fig. S9L–S9O, respectively).

Next, we evaluated the effect of the palbociclib/sabutoclax combination on leukemia progression in NSG mice injected with ALL-674 or ALL-1222 cells.

Treatment with palbociclib induced a moderate reduction in peripheral blood leukemia burden (17% and 32% decrease in ALL-674 and ALL-1222 samples, respectively), whereas treatment with sabutoclax had negligible effects. However, the combined treatment was significantly more effective than either drug alone (77% reduction for ALL-674, Fig. 7A and B and 90% reduction for ALL-1222, Fig. 7C and D) in suppressing leukemia load.

## Discussion

We show here that MYB expression is critically important for growth and leukemogenesis of Ph$^+$ ALL cells. Mechanistically, the effects of MYB depend on transcriptional regulation of many targets, among which, CDK6 and BCL2 are crucial mediators of its proliferative and antiapoptotic functions.

In addition to MYB-dependent regulation, several mechanisms may contribute to enhanced expression/activity of CDK6 in Ph$^+$

ALL. The CDK4/6 inhibitor INK4A is structurally altered in 30% to 50% of Ph$^+$ ALL (11, 52), the *CDK6* promoter is hypomethylated in BCR-ABL1–transformed cells (53), and miR-124 is epigenetically silenced in Ph$^+$ ALL, resulting in higher CDK6 levels (54). In addition to its kinase-dependent effects, CDK6 is also involved in transcriptional regulation (55, 56).

Silencing CDK6 (but not CDK4) alone suppressed S phase entry of Ph$^+$ ALL cells; however, this effect may not require kinase-independent mechanisms because it was undistinguishable from that induced by pharmacologic inhibition of CDK4/6. The essential role of CDK6 was noted in MLL-rearranged leukemias (57, 58), but no explanation was provided for the differential requirement of CDK4 and CDK6. Here, we show that CDK6 is readily detectable in the nucleus of Ph$^+$ ALL cells, whereas CDK4 is almost exclusively cytoplasmic. The exclusion of CDK4 from the nucleus likely explains its inability to compensate for the growth inhibition induced by CDK6 downregulation because expression of a nucleus-localized form of CDK4, in combination with cyclin D3 expression, partially rescued the impaired proliferation of MYB-silenced cells.

We do not know the reasons for the lack of nuclear import of CDK4 in Ph$^+$ ALL cells. A possible explanation might reside in the expression levels of different cyclin D proteins because CDK4 appears to interact preferentially with cyclin D1, whereas CDK6 binds preferentially to cyclin D3 (59) and levels of cyclin D3 mRNA are much higher than those of cyclin D1 in BV173 and SUP-B15 cells, based on microarray data. This may affect both nuclear import and kinase activity of CDK4.

Interestingly, MYB expression is required for leukemogenesis in a model of MLL-AF9 AML (22) and MLL-rearranged ALL, and AML cells are also dependent on CDK6 but not on CDK4 expression (57, 58). Furthermore, MYB and CDK6 expression is highly correlated in ALL and in adult AML, suggesting that MYB might link different oncogenic pathways to the activation of CDK6 expression.

Decreased susceptibility to apoptosis mediated by BCL2 is also important for MYB-dependent regulation of Ph$^+$ ALL cell growth. However, even in combination with CDK6/Cyclin D3, BCL2 enabled MYB-deficient BV173 cells to develop leukemia only after long latency, suggesting that other MYB-regulated pathways are important for a complete recovery of the leukemogenic potential of these cells.

A critical mechanism whereby MYB regulates gene expression is through its interaction with p300/CBP, because mutations of MYB in the p300/CBP-binding sites phenocopy the impaired hematopoiesis induced by MYB knockout and prevent leukemia formation (46–48). The MYB–p300 interaction seems necessary for CDK6 expression and cell-cycle progression but not for regulation of BCL2 expression and cell survival. Thus, drugs that disrupt this interaction might have limited efficacy in Ph$^+$ ALL unless MYB-regulated antiapoptotic pathway effects are also targeted.

Our approach of simultaneously inhibiting MYB-dependent proliferative and antiapoptotic programs recapitulates more faithfully the effects of MYB silencing in Ph$^+$ ALL, as indicated by the more potent suppression of *ex vivo* and *in vivo* cell growth by combining palbociclib with venetoclax or sabutoclax. Of interest, venetoclax treatment of patient-derived Ph$^+$ ALL cells revealed sample-to-sample variations in induction of apoptosis. These findings likely depend on the expression profile of BCL2 family members and suggest that the choice of a particular BCL2 antagonist in the clinic should be guided by the pattern of BCL2 family expression and the *ex vivo* drug sensitivity of Ph$^+$ leukemia cells from individual patients.

On the other hand, given that CDK4 is dispensable in Ph$^+$ ALL, CDK6-selective inhibitors might prove as effective as dual CDK4/6 inhibitors in blocking the proliferation of Ph+ ALL cells and may cause fewer side effects in normal cells.

In conclusion, our data indicate that targeting CDK6 and BCL2 is an effective strategy to exploit therapeutically the MYB addiction of Ph$^+$ ALL cells and might provide an alternative treatment for patients who develop resistance to TKI-based therapies.

## Disclosure of Potential Conflicts of Interest

G. Martinelli is a consultant/advisory board member for Abbvie, Incyte, Jazz Pharma, J&G, and Pfizer. No potential conflicts of interest were disclosed by the other authors.

## Authors' Contributions

**Conception and design:** M. De Dominici, B. Calabretta
**Development of methodology:** M. De Dominici, S. Addya
**Acquisition of data (provided animals, acquired and managed patients, provided facilities, etc.):** M. De Dominici, P. Porazzi, A.R. Soliera, P. Fortina, O. Spinelli, A. Rambaldi, A. Ferrari
**Analysis and interpretation of data (e.g., statistical analysis, biostatistics, computational analysis):** M. De Dominici, S.A. Mariani, S. Addya, P. Fortina, G. Martinelli, B. Calabretta
**Writing, review, and/or revision of the manuscript:** M. De Dominici, P. Porazzi, S. Addya, O. Spinelli, B. Calabretta
**Administrative, technical, or material support (i.e., reporting or organizing data, constructing databases):** M. De Dominici, P. Fortina, L.F. Peterson, A. Ferrari
**Study supervision:** M. De Dominici, P. Fortina, B. Calabretta
**Other (provided patient samples):** I. Iacobucci

## Acknowledgments

This work was supported by NCI grant RO1-CA167169 (B. Calabretta).

We thank Drs. A.M. Mazo and C.M. Eischen for critically reviewing the article and V. Minieri for edits to the text. We thank Drs. S.B. McMahon, T.L. Manser, and A.E. Aplin for helpful discussions and sharing of materials throughout the project. We thank Dr. M. Caliguri from the Ohio State University and Dr. M. Carrol from the Stem Cell and Xenograft Core of the University of Pennsylvania for providing primary Ph$^+$ ALL samples. We thank Dr. N. Flomenberg and the Bone Marrow Transplantation unit at Thomas Jefferson University for providing CD34$^+$ human hematopoietic progenitor cells. We thank Pfizer for kindly providing palbociclib and Dr. T. Gonda for kindly providing the pLVTSH-MYB shRNA vector. We also thank C. Kugel, E. Greenawalt, and R. DeRita for their help in obtaining preliminary results.

The costs of publication of this article were defrayed in part by the payment of page charges. This article must therefore be hereby marked *advertisement* in accordance with 18 U.S.C. Section 1734 solely to indicate this fact.

Received August 30, 2017; revised October 25, 2017; accepted December 8, 2017; published OnlineFirst December 12, 2017.

## References

1. Rowe JM, Buck G, Burnett AK, Chopra R, Wiernik PH, Richards SM, et al. Induction therapy for adults with acute lymphoblastic leukemia: results of more than 1500 patients from the international ALL trial: MRC UKALL XII/ECOG E2993. Blood 2005;106:3760–7.

2. Dores GM, Devesa SS, Curtis RE, Linet MS, Morton LM. Acute leukemia incidence and patient survival among children and adults in the United States, 2001–2007. Blood 2012;119:34–43.
3. Pulte D, Jansen L, Gondos A, Katalinic A, Barnes B, Ressing M, et al. Survival of adults with acute lymphoblastic leukemia in Germany and the United States. PloS One 2014;9:e85554.
4. Gleissner B, Gokbuget N, Bartram CR, Janssen B, Rieder H, Janssen JW, et al. Leading prognostic relevance of the BCR-ABL translocation in adult acute B-lineage lymphoblastic leukemia: a prospective study of the German Multicenter Trial Group and confirmed polymerase chain reaction analysis. Blood 2002;99:1536–43.
5. Wetzler M, Dodge RK, Mrozek K, Carroll AJ, Tantravahi R, Block AW, et al. Prospective karyotype analysis in adult acute lymphoblastic leukemia: the cancer and leukemia Group B experience. Blood 1999; 93:3983–93.
6. Fielding AK, Rowe JM, Richards SM, Buck G, Moorman AV, Durrant IJ, et al. Prospective outcome data on 267 unselected adult patients with Philadelphia chromosome-positive acute lymphoblastic leukemia confirms superiority of allogeneic transplantation over chemotherapy in the pre-imatinib era: results from the International ALL Trial MRC UKALLXII/ECOG2993. Blood 2009;113:4489–96.
7. Yanada M, Takeuchi J, Sugiura I, Akiyama H, Usui N, Yagasaki F, et al. High complete remission rate and promising outcome by combination of imatinib and chemotherapy for newly diagnosed BCR-ABL-positive acute lymphoblastic leukemia: a phase II study by the Japan Adult Leukemia Study Group. J Clin Oncol 2006;24:460–6.
8. Soverini S, De Benedittis C, Papayannidis C, Paolini S, Venturi C, Iacobucci I, et al. Drug resistance and BCR-ABL kinase domain mutations in Philadelphia chromosome-positive acute lymphoblastic leukemia from the imatinib to the second-generation tyrosine kinase inhibitor era: The main changes are in the type of mutations, but not in the frequency of mutation involvement. Cancer 2014;120:1002–9.
9. Calabretta B, Perrotti D. The biology of CML blast crisis. Blood 2004; 103:4010–22.
10. Williams RT, Sherr CJ. The INK4-ARF (CDKN2A/B) locus in hematopoiesis and BCR-ABL-induced leukemias. Cold Spring Harbor Symposia Quantit Biol 2008;73:461–7.
11. Mullighan CG, Miller CB, Radtke I, Phillips LA, Dalton J, Ma J, et al. BCR-ABL1 lymphoblastic leukaemia is characterized by the deletion of Ikaros. Nature 2008;453:110–4.
12. Feldhahn N, Henke N, Melchior K, Duy C, Soh BN, Klein F, et al. Activation-induced cytidine deaminase acts as a mutator in BCR-ABL1-transformed acute lymphoblastic leukemia cells. J Exp Med 2007;204:1157–66.
13. Klemm L, Duy C, Iacobucci I, Kuchen S, von Levetzow G, Feldhahn N, et al. The B cell mutator AID promotes B lymphoid blast crisis and drug resistance in chronic myeloid leukemia. Cancer cell 2009;16:232–45.
14. Perrotti D, Cesi V, Trotta R, Guerzoni C, Santilli G, Campbell K, et al. BCR-ABL suppresses C/EBPalpha expression through inhibitory action of hnRNP E2. Nature Genet 2002;30:48–58.
15. Waldron T, De Dominici M, Soliera AR, Audia A, Iacobucci I, Lonetti A, et al. c-Myb and its target Bmi1 are required for p190BCR/ABL leukemogenesis in mouse and human cells. Leukemia 2012;26:644–53.
16. Chai SK, Nichols GL, Rothman P. Constitutive activation of JAKs and STATs in BCR-Abl-expressing cell lines and peripheral blood cells derived from leukemic patients. J Immunol 1997;159:4720–8.
17. Soliera AR, Lidonnici MR, Ferrari-Amorotti G, Prisco M, Zhang Y, Martinez RV, et al. Transcriptional repression of c-Myb and GATA-2 is involved in the biologic effects of C/EBPalpha in p210BCR/ABL-expressing cells. Blood 2008;112:1942–50.
18. Lidonnici MR, Corradini F, Waldron T, Bender TP, Calabretta B. Requirement of c-Myb for p210(BCR/ABL)-dependent transformation of hematopoietic progenitors and leukemogenesis. Blood 2008;111:4771–9.
19. Ratajczak MZ, Hijiya N, Catani L, DeRiel K, Luger SM, McGlave P, et al. Acute- and chronic-phase chronic myelogenous leukemia colony-forming units are highly sensitive to the growth inhibitory effects of c-myb antisense oligodeoxynucleotides. Blood 1992;79:1956–61.
20. Calabretta B, Sims RB, Valtieri M, Caracciolo D, Szczylik C, Venturelli D, et al. Normal and leukemic hematopoietic cells manifest differential sensitivity to inhibitory effects of c-myb antisense oligodeoxynucleotides: an in vitro study relevant to bone marrow purging. Proc Natl Acad Sci USA 1991;88:2351–5.
21. Lahortiga I, De Keersmaecker K, Van Vlierberghe P, Graux C, Cauwelier B, Lambert F, et al. Duplication of the MYB oncogene in T cell acute lymphoblastic leukemia. Nature Genet 2007;39:593–5.
22. Zuber J, Rappaport AR, Luo W, Wang E, Chen C, Vaseva AV, et al. An integrated approach to dissecting oncogene addiction implicates a Myb-coordinated self-renewal program as essential for leukemia maintenance. Genes Dev 2011;25:1628–40.
23. Bujnicki T, Wilczek C, Schomburg C, Feldmann F, Schlenke P, Muller-Tidow C, et al. Inhibition of Myb-dependent gene expression by the sesquiterpene lactone mexicanin-I. Leukemia 2012;26:615–22.
24. Guzman ML, Rossi RM, Karnischky L, Li X, Peterson DR, Howard DS, et al. The sesquiterpene lactone parthenolide induces apoptosis of human acute myelogenous leukemia stem and progenitor cells. Blood 2005;105: 4163–9.
25. Kawasaki BT, Hurt EM, Kalathur M, Duhagon MA, Milner JA, Kim YS, et al. Effects of the sesquiterpene lactone parthenolide on prostate tumor-initiating cells: An integrated molecular profiling approach. Prostate 2009;69:827–37.
26. Uttarkar S, Dukare S, Bopp B, Goblirsch M, Jose J, Klempnauer KH. Naphthol AS-E phosphate inhibits the activity of the transcription factor Myb by blocking the interaction with the KIX domain of the coactivator p300. Mol Cancer Ther 2015;14:1276–85.
27. Uttarkar S, Dasse E, Coulibaly A, Steinmann S, Jakobs A, Schomburg C, et al. Targeting acute myeloid leukemia with a small molecule inhibitor of the Myb/p300 interaction. Blood 2016;127:1173–82.
28. Yang H, Chen D, Cui QC, Yuan X, Dou QP. Celastrol, a triterpene extracted from the Chinese "Thunder of God Vine," is a potent proteasome inhibitor and suppresses human prostate cancer growth in nude mice. Cancer Res 2006;66:4758–65.
29. Lee JH, Koo TH, Yoon H, Jung HS, Jin HZ, Lee K, et al. Inhibition of NF-kappa B activation through targeting I kappa B kinase by celastrol, a quinone methide triterpenoid. Biochem Pharmacol 2006;72:1311–21.
30. Young L, Sung J, Stacey G, Masters JR. Detection of mycoplasma in cell cultures. Nat Protoc 2010;5:929–34.
31. Drabsch Y, Hugo H, Zhang R, Dowhan DH, Miao YR, Gewirtz AM, et al. Mechanism of and requirement for estrogen-regulated MYB expression in estrogen-receptor-positive breast cancer cells. Proc Natl Acad Sci USA 2007;104:13762–7.
32. Corradini F, Cesi V, Bartella V, Pani E, Bussolari R, Candini O, et al. Enhanced proliferative potential of hematopoietic cells expressing degradation-resistant c-Myb mutants. J Biol Chem 2005;280:30254–62.
33. Corradini F, Bussolari R, Cerioli D, Lidonnici MR, Calabretta B. A degradation-resistant c-Myb mutant cooperates with Bcl-2 in enhancing proliferative potential and survival of hematopoietic cells. Blood Cells Mol Dis 2007;39:292–6.
34. Chou TC, Talalay P. Quantitative analysis of dose-effect relationships: the combined effects of multiple drugs or enzyme inhibitors. Adv Enzyme Regulation 1984;22:27–55.
35. Ito M, Hiramatsu H, Kobayashi K, Suzue K, Kawahata M, Hioki K, et al. NOD/SCID/gamma(c)(null) mouse: an excellent recipient mouse model for engraftment of human cells. Blood 2002;100:3175–82.
36. Schmitz NM, Hirt A, Aebi M, Leibundgut K. Limited redundancy in phosphorylation of retinoblastoma tumor suppressor protein by cyclin-dependent kinases in acute lymphoblastic leukemia. Am J Pathol 2006; 169:1074–9.
37. Takaki T, Fukasawa K, Suzuki-Takahashi I, Semba K, Kitagawa M, Taya Y, et al. Preferences for phosphorylation sites in the retinoblastoma protein of D-type cyclin-dependent kinases, Cdk4 and Cdk6, in vitro. J Biochem 2005;137:381–6.
38. Anders L, Ke N, Hydbring P, Choi YJ, Widlund HR, Chick JM, et al. A systematic screen for CDK4/6 substrates links FOXM1 phosphorylation to senescence suppression in cancer cells. Cancer cell 2011;20:620–34.
39. Roe JS, Mercan F, Rivera K, Pappin DJ, Vakoc CR. BET bromodomain inhibition suppresses the function of hematopoietic transcription factors in acute myeloid leukemia. Mol Cell 2015;58:1028–39.
40. Hirabayashi S, Ohki K, Nakabayashi K, Ichikawa H, Momozawa Y, Okamura K, et al. ZNF384-related fusion genes define a subgroup of childhood B-cell precursor acute lymphoblastic leukemia with a characteristic immunotype. Haematologica 2017;102:118–29.
41. Kang H, Chen IM, Wilson CS, Bedrick EJ, Harvey RC, Atlas SR, et al. Gene expression classifiers for relapse-free survival and minimal residual disease

improve risk classification and outcome prediction in pediatric B-precursor acute lymphoblastic leukemia. Blood 2010;115:1394–405.
42. Taylor D, Badiani P, Weston K. A dominant interfering Myb mutant causes apoptosis in T cells. Genes Dev 1996;10:2732–44.
43. Frampton J, Ramqvist T, Graf T. v-Myb of E26 leukemia virus up-regulates bcl-2 and suppresses apoptosis in myeloid cells. Genes Dev 1996;10: 2720–31.
44. Salomoni P, Perrotti D, Martinez R, Franceschi C, Calabretta B. Resistance to apoptosis in CTLL-2 cells constitutively expressing c-Myb is associated with induction of BCL-2 expression and Myb-dependent regulation of bcl-2 promoter activity. Proc Natl Acad Sci USA 1997;94:3296–301.
45. Jing D, Bhadri VA, Beck D, Thoms JA, Yakob NA, Wong JW, et al. Opposing regulation of BIM and BCL2 controls glucocorticoid-induced apoptosis of pediatric acute lymphoblastic leukemia cells. Blood 2015;125:273–83.
46. Sandberg ML, Sutton SE, Pletcher MT, Wiltshire T, Tarantino LM, Hogenesch JB, et al. c-Myb and p300 regulate hematopoietic stem cell proliferation and differentiation. Dev Cell 2005;8:153–66.
47. Papathanasiou P, Tunningley R, Pattabiraman DR, Ye P, Gonda TJ, Whittle B, et al. A recessive screen for genes regulating hematopoietic stem cells. Blood 2010;116:5849–58.
48. Pattabiraman DR, McGirr C, Shakhbazov K, Barbier V, Krishnan K, Mukhopadhyay P, et al. Interaction of c-Myb with p300 is required for the induction of acute myeloid leukemia (AML) by human AML oncogenes. Blood 2014;123:2682–90.
49. Nemoto A, Saida S, Kato I, Kikuchi J, Furukawa Y, Maeda Y, et al. Specific antileukemic activity of PD0332991, a CDK4/6 Inhibitor, against Philadelphia chromosome-positive lymphoid leukemia. Mol Cancer Ther 2016;15:94–105.
50. Souers AJ, Leverson JD, Boghaert ER, Ackler SL, Catron ND, Chen J, et al. ABT-199, a potent and selective BCL-2 inhibitor, achieves antitumor activity while sparing platelets. Nature Med 2013;19:202–8.
51. Wei J, Stebbins JL, Kitada S, Dash R, Placzek W, Rega MF, et al. BI-97C1, an optically pure Apogossypol derivative as pan-active inhibitor of antiapoptotic B-cell lymphoma/leukemia-2 (Bcl-2) family proteins. J Med Chem 2010;53:4166–76.
52. Iacobucci I, Ferrari A, Lonetti A, Papayannidis C, Paoloni F, Trino S, et al. CDKN2A/B alterations impair prognosis in adult BCR-ABL1-positive acute lymphoblastic leukemia patients. Clin Cancer Res 2011;17:7413–23.
53. Kollmann K, Heller G, Ott RG, Scheicher R, Zebedin-Brandl E, Schneckenleithner C, et al. c-JUN promotes BCR-ABL-induced lymphoid leukemia by inhibiting methylation of the 5' region of Cdk6. Blood 2011;117: 4065–75.
54. Agirre X, Vilas-Zornoza A, Jimenez-Velasco A, Martin-Subero JI, Cordeu L, Garate L, et al. Epigenetic silencing of the tumor suppressor microRNA Hsa-miR-124a regulates CDK6 expression and confers a poor prognosis in acute lymphoblastic leukemia. Cancer Res 2009;69:4443–53.
55. Kollmann K, Heller G, Schneckenleithner C, Warsch W, Scheicher R, Ott RG, et al. A kinase-independent function of CDK6 links the cell cycle to tumor angiogenesis. Cancer cell 2016;30:359–60.
56. Scheicher R, Hoelbl-Kovacic A, Bellutti F, Tigan AS, Prchal-Murphy M, Heller G, et al. CDK6 as a key regulator of hematopoietic and leukemic stem cell activation. Blood 2015;125:90–101.
57. van der Linden MH, Willekes M, van Roon E, Seslija L, Schneider P, Pieters R, et al. MLL fusion-driven activation of CDK6 potentiates proliferation in MLL-rearranged infant ALL. Cell cycle (Georgetown, Tex) 2014;13:834–44.
58. Placke T, Faber K, Nonami A, Putwain SL, Salih HR, Heidel FH, et al. Requirement for CDK6 in MLL-rearranged acute myeloid leukemia. Blood 2014;124:13–23.
59. Spofford LS, Abel EV, Boisvert-Adamo K, Aplin AE. Cyclin D3 expression in melanoma cells is regulated by adhesion-dependent phosphatidylinositol 3-kinase signaling and contributes to G1-S progression. J Biol Chem 2006;281:25644–51.

Cancer Research
The Journal of Cancer Research (1916–1930) | The American Journal of Cancer (1931–1940)

AACR American Association for Cancer Research

# Targeting CDK6 and BCL2 Exploits the "MYB Addiction" of Ph$^+$ Acute Lymphoblastic Leukemia

Marco De Dominici, Patrizia Porazzi, Angela Rachele Soliera, et al.

*Cancer Res* 2018;78:1097-1109. Published OnlineFirst December 12, 2017.